

Interconversions among the $E\rightleftharpoons Z$ -Carotene Isomers: Theoretical Study

M. Darijani, M. Shahraki* and S.M. Habibi-Khorassani

Department of Chemistry, Faculty of Science, University of Sistan and Baluchestan, P. O. Box: 98135-674, Zahedan, Iran

(Received 5 August 2020, Accepted 31 October 2020)

The Minnesota functional, M062x, with 6-31+G(d,P) basis set has been employed to study interconversions among all- E -, 9 Z -, 13 Z - and 15 Z - β -carotene isomers. Calculations provided essential data concerning the thermodynamic stabilities, the rate constants, activation energies, and HOMO and LUMO of all $E\rightleftharpoons Z$ interconversions of β -carotene. The rate constants for the $E\rightleftharpoons Z$ interconversions have been obtained with the transition-state theory based on the potential energy surface. In terms of energy, all- E -isomer was more stable than the Z -isomers, and the formation of the 9 Z -isomer was the slowest interconversion. Raising the temperature increased the rate of interconversions. The tunneling effect was negligible, and it was not taken into account in determining the rate constant of the $E\rightleftharpoons Z$ interconversions.

Keywords: β -Carotene, Isomerism, Kinetics, Minnesota functionals, Tunneling effect

INTRODUCTION

Food chemistry deals with chemical processes, including the composition and properties of food and the chemical changes it undergoes during handling, processing, and storage. Food quality or safety can alter by external agents, such as heat, low pH, and light exposure [1,2]. Carotenoids as an important food colorants source are found in a variety of vegetables, summer crops, aquatic species, and plants. Due to the properties of carotenoids, these compounds have a wide range of applications in various food, industrial, pharmaceutical, and medical sciences [3-12]. One of the most well-known carotenoids is β -carotene that consists of 11 conjugated double bonds and a β -ring at each end of the chain. The study of interconversions among the $E\rightleftharpoons Z$ - β -carotene isomers is very significant in biological systems. These isomers exhibit different activities in the role of anti-cancer, antioxidant, and anti-atherosclerotic agents. β -Carotene is mainly present as all- E - β -carotene, and the 9 Z , 13 Z and 15 Z - β -carotenes are the most common

Z -isomers [13]. To understand and enhance the beneficial effects of carotenoids, it is necessary to study the effect of interconversions of $E\rightleftharpoons Z$ isomers on relevant functional changes. Numerous research activities have been performed on the conversion of β -carotene isomers [14-22]. In one of the oldest of these works, Doering *et al.* reported interconversions among $E\rightleftharpoons Z$ β -carotene isomers from a kinetic and thermodynamic point of view using NMR methods in a wide temperature range [19]. They confirmed the role of 15 Z - and 13 Z - β -carotenes as the anti-cancer agents. Guo *et al.* showed that the low-lying isomers of β -carotenes are in equilibrium with the all-trans isomers in the following order: all- E > 9 Z > 13 Z > 15 Z - β -carotenes by using density functional theory at the level of B3LYP/6-31G(d) on single and triplet states of the open shell. Also, they showed that the rotation barrier toward the 13 Z -isomer has the lowest energy [14]. In a computational study on the structural, energetic, and vibrational spectroscopic characteristics of β -carotene, Schlucker *et al.* employed the density functional theory [17]. The density functional theory method B3LYP was also employed to study the thermal interconversions of β -carotene by Qiu *et al.* [15]. They have shown the sequence of stability of neutral isomers is all- E > 9 Z > 13 Z > 9 Z , 13-di- Z = 9, 13'-di- Z > 15 Z > 9, 15-di- Z >

*Corresponding author. E-mail: mehdishahraki@chem.usb.ac.ir

13, 15-di-Z > 7Z > 11Z. Ceron-Carrasco *et al.* applied the combined density functional theory and configuration interaction method (DFT-MRCI) to explore the ground and low-lying electronically excited states of various β -carotenes [18]. The calculations revealed a correlation between the oscillator strengths of these transitions and the C6-C6' distance, and also explained the effect of the molecular configuration on the shape of the UV-Vis spectra. Moreover, kinetic studies of β -carotene degradation and interconversions were intensively investigated, and a first-order reaction with activation energies range from 20-171 kJ mol⁻¹ was reported [23]. The interconversion pathways were suggested to proceed *via* a triplet excited state or may be mediated by cation radical or dication formation either via the creation of diradical species [11]. Theoretical studies of the interconversions of β -carotenes are performed to investigate many items or details that are not observable by experimental methods. In this work, theoretical studies are performed on the interconversions among the *E*↔*Z*- β -carotene isomers using the M062x functional and 6-31+G(d,p) basis set *via* diradical species. In previous computational works, the main focus has been on the stability of isomers in their various states and the study of Raman and IR spectra. In some cases, *cis*-*trans* interconversions and activation parameters have been studied. In this work, the stability of more frequent isomers of β -carotenes and converting them to each other are investigated using DFT at the M06-2x level of theory. The transition state theory (TST), constant rate, tunneling effects and quasi rigid-rotor-harmonic-oscillator (qRRHO) correction are also employed.

COMPUTATIONAL METHODS

All calculations were performed using the Gaussian 16 program. Optimization and vibrational analysis of the stationary points were performed using M062x/6-31g+(d,p) at 298.15 K [24,25]. M062x has been specifically developed for thermochemical kinetic studies providing the average absolute deviations from well-established experimental activation near 1 kcal mol⁻¹. This model has been shown to be accurate for predicting transition states for the treatment of general thermochemistry and kinetics. The M06-2X functional is also applicable for chemical kinetics studies

and is reliable for predicting energy barriers. Many isomerizations with this method have already been investigated and are of acceptable accuracy [26,32]. All transition states corresponding to the investigated pathways were obtained on the potential energy surface (PES) that identified by having one imaginary frequency in the Hessian matrix. It was established that transition states get in touch with the corresponding intermediates through the application of the eigenvector of the imaginary frequency and later optimization of the resulting structures. The tunneling correction to the rate constants was considered and computed with the wigner and Ekart method [33,34]. The diradical form of the structures was optimized at their triplet state. In the case of open-shell triplet electronic structures, calculations were done at the UM062x levels. Rate constants were calculated using conventional transition-state theory and Eq. (1),

$$k = \frac{k_B T}{h} e^{\frac{(G_{TS} - G_{react})}{RT}} \quad (1)$$

where k_B and h are the Boltzmann and plank constants.

The Kinetic and Statistical Thermodynamical Package (KiSThelP) software was used to compute each rate constant [35]. Stability check of wave functions was performed for all calculated structures, confirming stable wavefunctions. The quasi rigid-rotor-harmonic-oscillator (qRRHO) was used for entropic contributions of low-frequency modes that could further improve the calculated free energy. The qRRHO approximation was obtained *via* GoodVibes v. 2.0.3 [36].

RESULTS AND DISCUSSION

The optimized structures of neutral and diradical of all-*E*-, 9*Z*-, 13*Z*- and 15*Z*- β -carotenes are shown in Fig. 1. The absolute values of enthalpy, Gibbs free energies, and electronic energies (corrected with zero point energy) of all-*E*-and *Z*- β -carotenes are shown in Table 1. The result values increase in the order: 15*Z*- β -carotene > 13*Z*- > 9*Z*- > all-*E*- β -carotene. So, all-*E*- β -carotenes are more stable than 9*Z*, 13*Z*, 15*Z* and 9*Z*- β -carotene is more stable than other two *Z*-isomers. This trend is observed for neutral form. The order of the most stable isomers for the radical form is

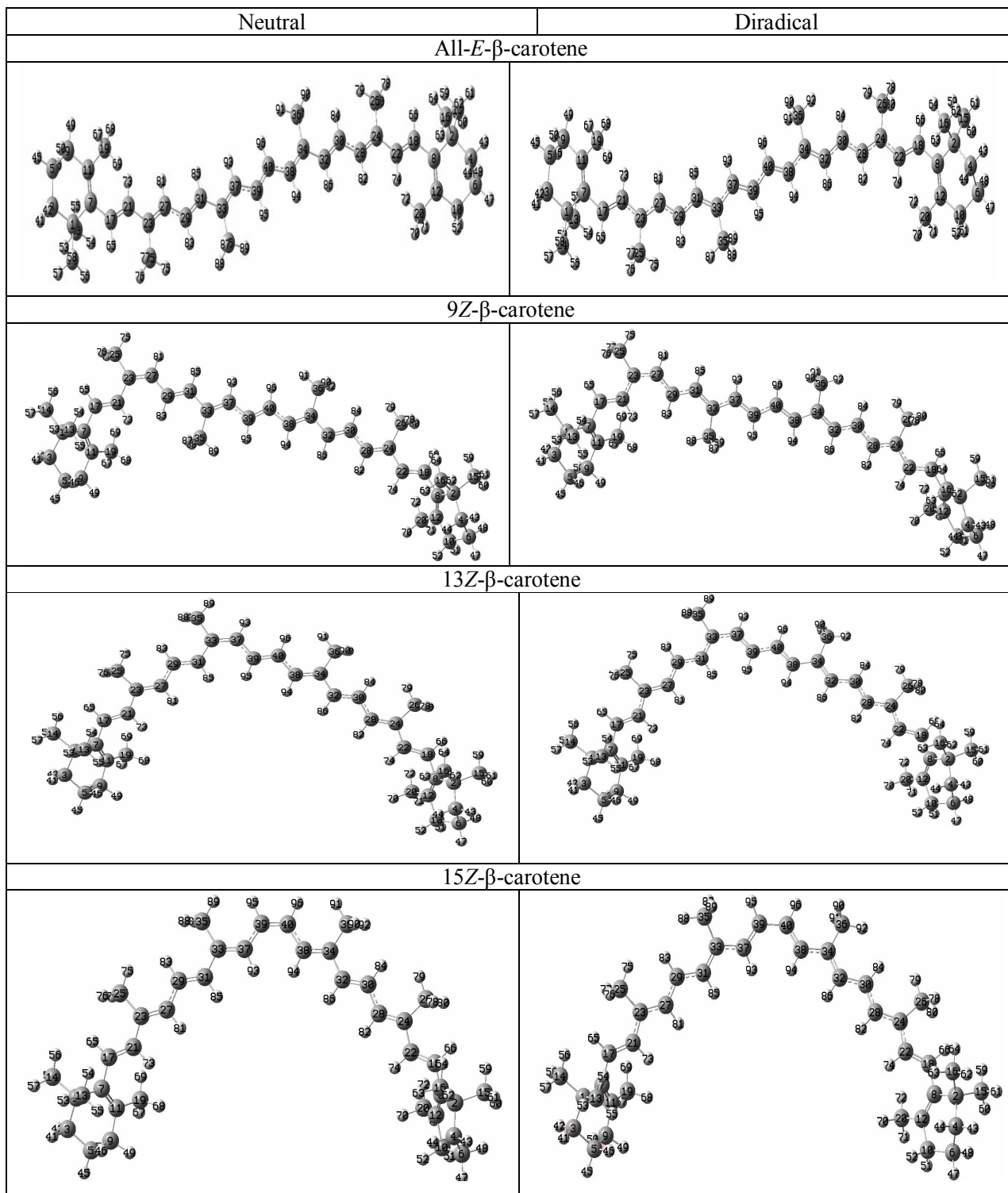


Fig. 1. Optimized structures of all-*E*, 9*Z*, 13*Z* and 15*Z*- β -carotenes in two neutral and diradical forms at the M062X/6-31+G(d) level.

Table 1. The Absolute Enthalpies, Gibbs Free Energies, and Electronic Energies (Corrected with Zero Point Energy) of all-*E*, 9*Z*, 13*Z*, 15*Z*- β -carotenes in Neutral and Diradical Forms. All Units are in kcal mol⁻¹

	Neutral		Diradical			
	E	H	G	E	H	G
All- <i>E</i> - β -carotene	-976644.03	-976614.83	-976697.15	-976625.07	-976595.74	-976678.68
9 <i>Z</i> - β -carotene	-976643.30	-976614.14	-976696.10	-976623.81	-976594.50	-976677.38
13 <i>Z</i> - β -carotene	-976643.12	-976613.97	-976695.97	-976622.28	-976592.81	-976676.69
15 <i>Z</i> - β -carotene	-976641.83	-976612.63	-976695.20	-976622.06	-976592.69	-976675.99

Table 1A. The Gibbs Free Energies (in kcal mol⁻¹) are Corrected with Refined Entropy Estimates Obtained by q-RRHO Approximation

	Neutral	Diradical
All- <i>E</i> - β -carotenes	-976694.75	-976676.50
9 <i>Z</i> - β -carotene	-976693.85	-976675.20
13 <i>Z</i> - β -carotene	-976693.73	-976674.34
15 <i>Z</i> - β -carotene	-976692.80	-976673.80

as follows: all-*E*- β -carotenes > 9*Z*- > 15*Z*- > 13*Z*- β -carotene. These results are in good agreement with the results calculated by Dan Qi at the B3LYP/6-31G* level of theory.

The free energy correction with the quasi-rigid-rotor-harmonic-oscillator (qRRHO) reported in Table 1A in the comparison with the value of free energy in Table 1 differs within 2.5 kcal mol⁻¹ from each other.

Some important bond lengths and dihedral angles of neutral and diradical of all-*E*, 9*Z*, 13*Z* and 15*Z*- β -carotenes are shown in Table 2. Two of the isoprene units are at the site of conversion to 9*Z*- and 13*Z*-isomers. Comparison of structural parameters in E-isomer shows that double bonds C₁₇-C₂₁ (0.01 Å) and C₂₉-C₃₁ (0.07 Å) increase and single bonds C₂₁-C₂₃ (0.03 Å) and C₃₁-C₃₃ (0.07 Å) decrease. The comparison of the structural parameters of the two isoprene units in the neutral and radical forms of the 9*Z*- and 13*Z*-isomers show that the changes in these bonds for the 13*Z*-

isomer are greater.

Frontier Molecular Orbital

The frontier molecular orbitals of all-*E*, 9*Z*, 13*Z* and 15*Z*- β -carotenes for neutral structures are shown in Fig. 2. For all isomers, the HOMOs are localized on the double bond, and LUMOs are localized on the single bond. The energies of HOMO, LUMO, and their orbital energy gaps are gathered in Table 3. The energy gaps between HOMO's and LUMO's for all-*E*- β -carotene are smaller than those for 9*Z*, 13*Z* and 15*Z*- β -carotenes, so all-*E*- β -carotene has high reactivity. Among three *Z*- β -carotenes, 9*Z*- has the smallest energy band gap.

Diradical structures with two unpaired electrons have two singly occupied molecular orbitals (SOMOs). SOMOs and LUMOs of all-*E*- β -carotene and three *Z*- β -carotenes are shown in Fig. 3 and Fig. S1, respectively. The SOMOs and SOMO⁻¹s are almost non-degenerate (-0.26000 and

Table 2. Selected Geometrical Parameters of all *E*-, 9*Z*, 13*Z*, 15*Z*- β -carotene in Two Forms: Neutral and Diradical (Bond Lengths in Å, Dihedral Angles in Degree)

	Neutral		Diradical	
	All- <i>E</i> - β -carotene	9 <i>Z</i> - β -carotene	All- <i>E</i> - β -carotene	9 <i>Z</i> - β -carotene
C ₁₇ -C ₂₁	1.34617	1.34645	1.35886	1.35499
C ₂₁ -C ₂₃	1.46125	1.46105	1.43729	1.44273
C ₂₃ -C ₂₇	1.35718	1.35776	1.39249	1.38866
C ₂₇ -C ₂₉	1.44608	1.44818	1.39657	1.40390
C ₂₇ -H ₈₁	1.09055	1.09011	1.09092	1.09042
C ₂₁ -C ₂₃ -C ₂₇ -C ₂₉	-179.78035	0.32950	179.82565	0.15367
C ₂₉ -C ₂₇ -C ₂₃ -C ₂₅	0.01397	-179.62530	-0.29360	-179.89665
C ₂₁ -C ₂₃ -C ₂₇ -H ₈₁	0.09610	-179.93704	-0.06535	-179.95235
		13 <i>Z</i> - β -carotene		13 <i>Z</i> - β -carotene
C ₂₉ -C ₃₁	1.35346	1.35268	1.41508	1.40125
C ₃₁ -C ₃₃	1.45384	1.45447	1.37677	1.38642
C ₃₃ -C ₃₇	1.36015	1.36076	1.44659	1.44494
C ₃₇ -H ₉₃	1.09045	1.08996	1.09058	1.09054
C ₃₃ -C ₃₅	1.50541	1.50712	1.50348	1.50842
C ₃₁ -C ₃₃ -C ₃₇ -C ₃₉	-179.66327	-0.16754	179.93010	-10.88722
C ₃₅ -C ₃₃ -C ₃₇ -C ₃₉	0.23776	179.93285	-0.05256	169.34908
C ₃₅ -C ₃₃ -C ₃₇ -H ₉₃	0.19490	179.81198	179.95931	-9.63064
		15 <i>Z</i> - β -carotene		15 <i>Z</i> - β -carotene
C ₃₇ -C ₃₉	1.44164	1.44192	1.35616	1.35572
C ₃₈ -C ₄₀	1.35605	1.35592	1.35639	1.35589
C ₃₉ -C ₄₀	1.35605	1.35980	1.44575	1.45710
C ₄₀ -H ₉₆	1.08808	1.08588	1.08921	1.08808
C ₃₉ -H ₉₅	1.08805	1.08587	1.08923	1.08809
C ₃₇ -C ₃₉ -C ₄₀ -C ₃₈	-179.71046	0.07933	179.95119	-23.25546
H ₉₅ -C ₃₉ -C ₄₀ -C ₃₈	0.15714	179.92985	-0.03790	158.06763
H ₉₆ -C ₄₀ -C ₃₉ -C ₃₇	0.16617	179.99079	-0.02767	158.20730
H ₉₅ -C ₃₉ -C ₄₀ -H ₉₆	179.96623	0.00000	179.98324	-20.46961

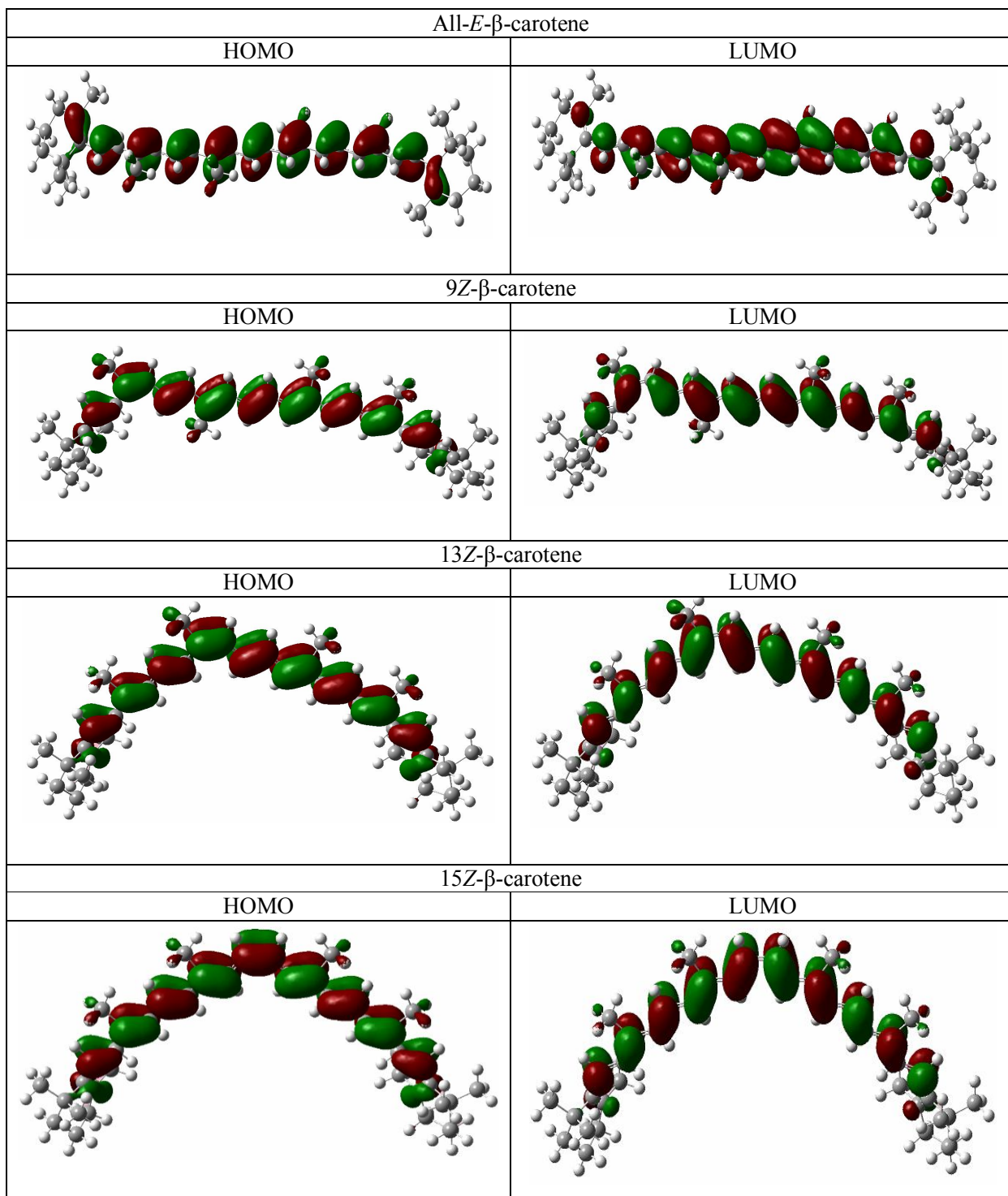


Fig. 2. HOMO and LUMO distributions of all-*E*, 9*Z*, 13*Z*, 15*Z*- β -carotenes obtained at the M062x/6-31+G(d,p) level.

Table 3. HOMO and LUMO Energies and HOMO-LUMO Energy Gaps (in a.u.) of all-*E*, 9*Z*, 13*Z*, 15*Z*- β -carotenes

	HOMO	LUMO	HOMO-LUMO
All- <i>E</i> - β -carotene	-0.21422	-0.06105	0.15317
9 <i>Z</i> - β -carotene	-0.21443	-0.05960	0.15483
13 <i>Z</i> - β -carotene	-0.21535	-0.05878	0.15657
15 <i>Z</i> - β -carotene	-0.21579	-0.05968	0.15611

Table 4. SOMO, SOMO⁻¹ and LUMO Energies (in a.u.) of all *E*, 9*Z*, 13*Z*, 15*Z*- β -carotenes Form Diradical

	SOMO	SOMO ⁻¹	LUMO
All- <i>E</i> - β -carotenes	-0.26000	-0.23716	-0.09287
9 <i>Z</i> - β -carotene	-0.26070	-0.23814	-0.09240
13 <i>Z</i> - β -carotene	-0.25917	-0.23702	-0.09405
15 <i>Z</i> - β -carotene	-0.25930	-0.23854	-0.09172

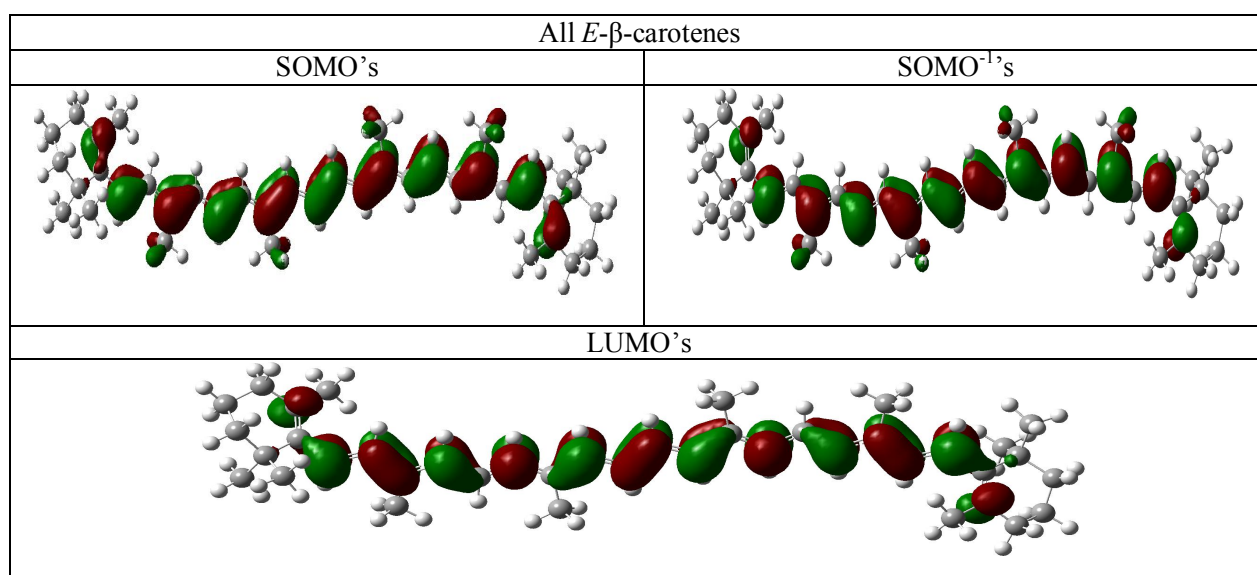


Fig. 3. SOMOs and LUMOs distributions of all-*E*- β -carotenes form diradical.

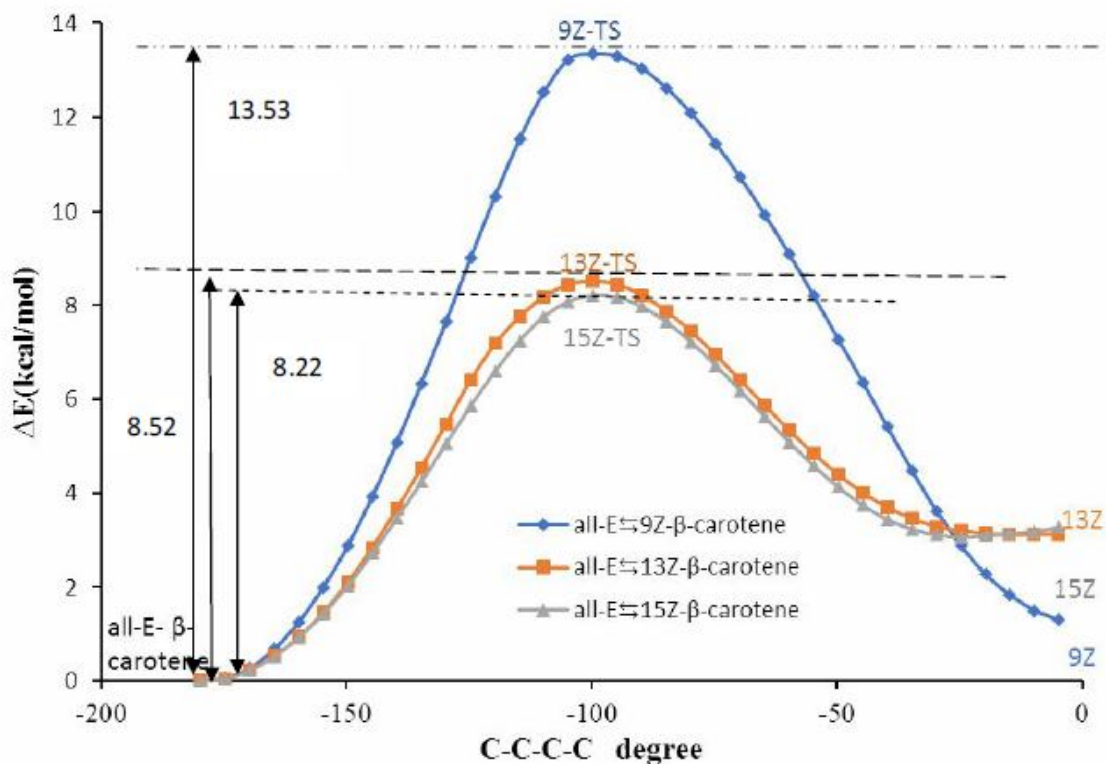


Fig. 4. Potential energy profile along the coordinates $C_{21}-C_{23}-C_{27}-C_{29}$, $C_{31}-C_{33}-C_{37}-C_{39}$, $C_{37}-C_{39}-C_{40}-C_{38}$ starting from conversions of *E*- to *Z*- β -carotenes in diradical form.

-0.23716 a.u.). Obviously, SOMOs and SOMO⁻¹s occupy different parts of space with a small shared region. The energies of SOMOs are reported in Table 4.

Interconversions via Diradical

Potential energy profile along with the rotation around $C_{21}-C_{23}-C_{27}-C_{29}$, $C_{31}-C_{33}-C_{37}-C_{39}$ and $C_{37}-C_{39}-C_{40}-C_{38}$ dihedral angles for the formation of 9Z, 13Z and 15Z- β -carotenes is shown in Fig. 4. The maximum in the potential energy surface is the transition state (*TS*) structures, and all-*E*- and *Z*-isomers are regarded as starting geometry. The *TS* structures and their imaginary frequencies for the *E*↔*Z* interconversions of the β -carotene are shown in Fig. 5. The energy of the rotation barriers for the path of conversion of all-*E* to *Z*- through 9Z-*TS*, 13Z-*TS* and 15Z-*TS* are 13.35, 8.53 and 8.22 kcal mol⁻¹, respectively, and in return path are 12.09, 5.42 and 5.02 kcal mol⁻¹, respectively.

Some important bond lengths and dihedral angles of all-*E*- β -carotenes, 9Z-*TS*, 13Z-*TS* and 15Z-*TS* are reported in

Table 5. The values of the responsible dihedral angles $C_{21}-C_{23}-C_{27}-C_{29}$, $C_{31}-C_{33}-C_{37}-C_{39}$, $C_{37}-C_{39}-C_{40}-C_{38}$ in the three interconversions for the transition states are around 98-99°. During these interconversions, the lengths of important bonds $C_{23}-C_{27}$, $C_{33}-C_{37}$, $C_{39}-C_{40}$ increase with the change of *E*-isomer to the transition state and the amounts of neighboring bonds $C_{17}-C_{21}$, $C_{29}-C_{31}$ increase, and the bonds $C_{21}-C_{23}$, $C_{31}-C_{33}$ decrease.

The S^2 value is often used as a measure of the spin contamination of unrestricted open-shell calculations. For a diradical with multiplicity of three, the value should be 2. Any deviation from this value is due to spin contamination. The results of $\langle S^2 \rangle$ are given in Table 6. Some studies have assumed that if the predicted value deviates by less than 10% from its theoretical value, the effects of spin contamination are negligible [37]. The deviation values are in a range from 4.92-6.55%. Therefore, the spin contamination is not severe.

The unimolecular kinetic rate constants of *E*↔*Z*

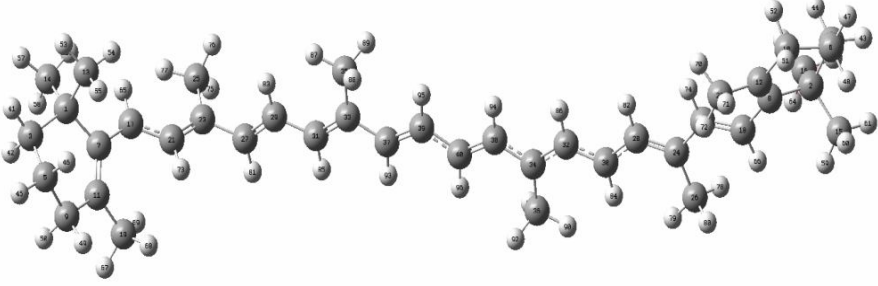
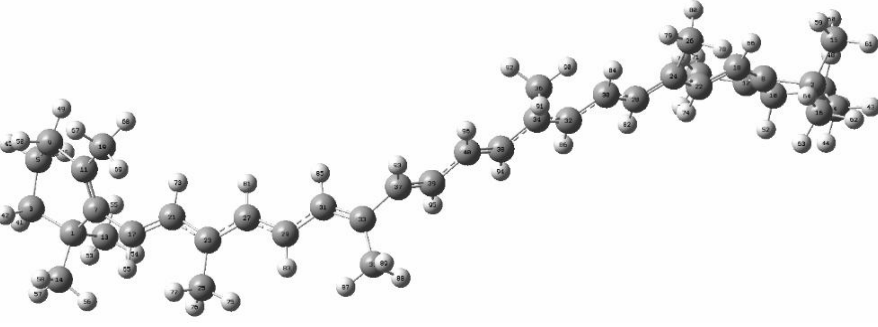
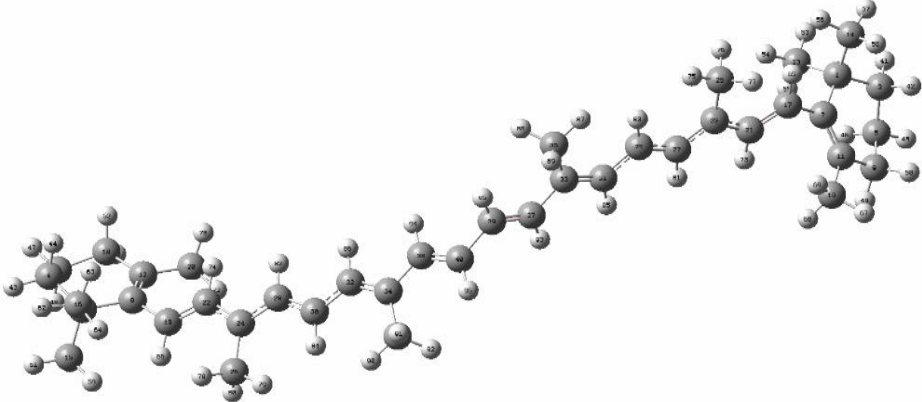
	104.26i	9Z-TS
	90.82i	13Z-TS
	125.60 i	15Z-TS

Fig. 5. Transition state structures and their imaginary frequencies (cm^{-1}) for the $E \rightleftharpoons Z$ interconversions of β -carotenes in diradical form.

interconversions estimated by TST theory [38,39], and the activation parameters for interconversions are summarized in Table 7. The values of Gibbs free activation energies for the $E \rightleftharpoons 9Z$, $E \rightleftharpoons 13Z$ and $E \rightleftharpoons 15Z$ - β -carotenes interconversions are 12.61, 7.52 and 7.85 kcal mol^{-1} , respectively. The $E \rightleftharpoons 9Z$, in comparison with other interconversions, has more considerable Gibbs free activation energies. Moreover, 9Z- β -carotene is more stable than 13Z- and 15Z- β -carotenes. Considering the rate

constant given in Table 7, it can be found that the rate constant calculated for the $E \rightleftharpoons 13Z$ - β -carotene interconversion is highest. The $E \rightleftharpoons 13Z$ interconversion has a more positive value of activation entropy and greater activation enthalpy with respect to the $E \rightleftharpoons 15Z$ - β -carotene interconversion.

The constant rate calculations are performed in the temperature range of 298-498 K. Temperature dependence of the rate constants computed for the $E \rightleftharpoons Z$ - β -carotenes

Table 5. Selected Geometrical Parameters of all-*E*- β -carotenes, 9*Z*-*TS*, 13*Z*-*TS*, and 15*Z*-*TS* i. Bond Lengths are in Å and Dihedral Angles are in Degree

	All <i>E</i> - β -carotene	9 <i>Z</i> - β -carotene
C ₁₇ -C ₂₁	1.35886	1.40712
C ₂₁ -C ₂₃	1.43729	1.37813
C ₂₃ -C ₂₇	1.39249	1.48474
C ₂₇ -C ₂₉	1.39657	1.34536
C ₂₇ -H ₈₁	1.09092	1.09371
C ₂₁ -C ₂₃ -C ₂₇ -C ₂₉	179.82565	-98.53037
C ₂₉ -C ₂₇ -C ₂₃ -C ₂₅	-0.29360	82.14488
C ₂₁ -C ₂₃ -C ₂₇ -H ₈₁	-0.06535	83.22668
	All <i>E</i> - β -carotene	13 <i>Z</i> - β -carotene
C ₂₉ -C ₃₁	1.41508	1.43168
C ₃₁ -C ₃₃	1.37677	1.35963
C ₃₃ -C ₃₇	1.44659	1.48692
C ₃₇ -H ₉₃	1.09058	1.09265
C ₃₃ -C ₃₅	1.50348	1.50525
C ₃₁ -C ₃₃ -C ₃₇ -C ₃₉	179.93010	-99.79811
C ₃₅ -C ₃₃ -C ₃₇ -C ₃₉	-0.05256	81.10435
C ₃₅ -C ₃₃ -C ₃₇ -H ₉₃	179.95931	-97.13985
	All <i>E</i> - β -carotenes	15 <i>Z</i> - β -carotene
C ₃₇ -C ₃₉	1.35616	1.34924
C ₃₈ -C ₄₀	1.35639	1.34930
C ₃₉ -C ₄₀	1.44575	1.48202
C ₄₀ -H ₉₆	1.08921	1.09031
C ₃₉ -H ₉₅	1.08923	1.09034
C ₃₇ -C ₃₉ -C ₄₀ -C ₃₈	179.95119	-98.45376
H ₉₅ -C ₃₉ -C ₄₀ -C ₃₈	-0.03790	82.43439
H ₉₆ -C ₄₀ -C ₃₉ -C ₃₇	-0.02767	82.42896
H ₉₅ -C ₃₉ -C ₄₀ -H ₉₆	179.98324	0.00000

Table 6. The Results of $\langle S^2 \rangle$ Obtained with Unrestricted Open-shell Calculations for all-*E*- β -Carotenes, Three *Z* Isomers and 9*Z*-TS, 13*Z*-TS and 15*Z*-TS

	$\langle S^2 \rangle$
All- <i>E</i> - β -carotenes	2.1011
9 <i>Z</i> - β -carotene	2.0984
13 <i>Z</i> - β -carotene	2.1016
15 <i>Z</i> - β -carotene	2.1046
9 <i>Z</i> -TS	2.1307
13 <i>Z</i> -TS	2.1313
15 <i>Z</i> -TS	2.1310

Table 7. Activation Parameters and Rate Constants for the *E* \rightleftharpoons *Z*- β -Carotenes Interconversions at 298.0 K

	<i>E</i> \rightleftharpoons 9 <i>Z</i>	<i>E</i> \rightleftharpoons 13 <i>Z</i>	<i>E</i> \rightleftharpoons 15 <i>Z</i>
ΔH^\ddagger (kcal mol ⁻¹)	12.33(13.7) ^a	7.51(9.5) ^a	7.31(10.0) ^a
ΔS^\ddagger (cal mol ⁻¹ K ⁻¹)	-0.93	-0.05	-1.81
ΔG^\ddagger (kcal mol ⁻¹)	12.61(12.8) ^a	7.52(8.6) ^a	7.85(9.0) ^a
ΔG^\ddagger (kcal mol ⁻¹) ^b	12.59	7.60	7.79
k (s ⁻¹)	3.5126×10^3	1.8877×10^7	1.0893×10^7

^aB3LYP/6-31G(d) [14]. ^bGibbs free activation energy correction with qRRHO approximation.

interconversions of reactions are plotted in Fig. 6. The rate constant for the conversion of the *E* to 9*Z*-isomer increases gradually with increasing temperature, but for the conversion of the *E*- to 13*Z*-isomer with increasing temperature, the rate constant increases with a steeper slope, because the Gibbs free activation energy of the *E* \rightleftharpoons 9*Z* interconversions is greater than that of the *E* \rightleftharpoons 13*Z* interconversions. The enthalpy and Gibbs free activation energy of our result were obtained, lower than those previously reported by Wen-HsinGuo for all interconversions the same prediction of the order obtained for their activities.

The tunneling coefficients for the *E* \rightleftharpoons *Z*- β -carotenes interconversions are computed with the Wigner and Ekart method, and the effect of temperature is assessed by Wigner method. Tunneling corrections and rate constants with tunneling effect are tabulated in Table 8. Comparing the values of the calculated rate constants with and without the tunneling effects shows that the tunneling effects are insignificant and negligible.

The tunneling effect of 15*Z* is more significant than that of 9*Z* and 13*Z*. The tunneling coefficients are nearly between 1-1.02 unities for the *E* \rightleftharpoons *Z*- β -carotenes interconversions and increase as the temperature decreases.

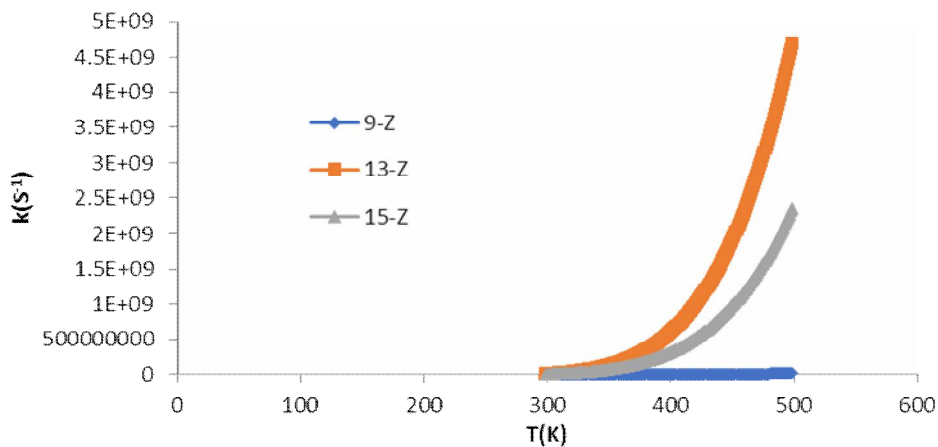


Fig. 6. Temperature dependence of rate constants for the $E \rightleftharpoons Z$ - β -carotenes interconversions.

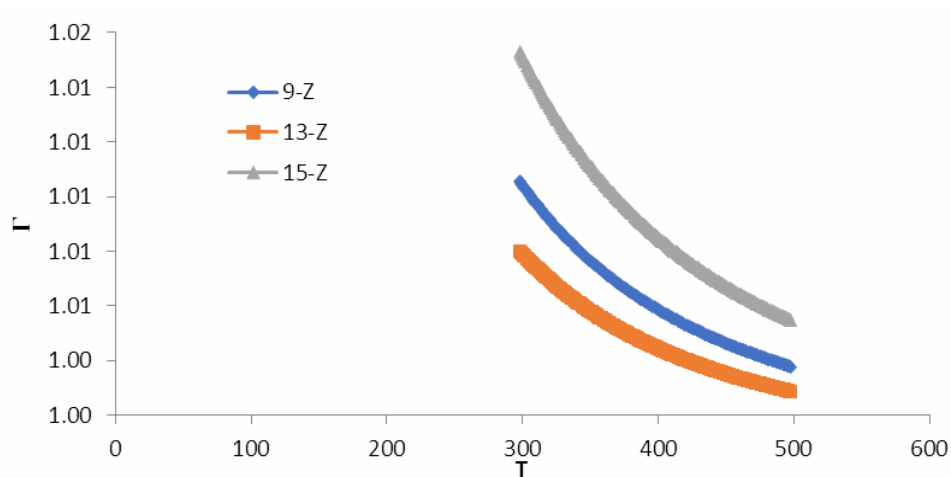


Fig. 7. The Wigner-based tunneling coefficients calculated for the $E \rightleftharpoons Z$ - β -carotenes.

Table 8. Comparison of the Tunneling Corrections for Three Interconversions Using the Wigner's Approach and Eckart Method

Step	Tunnelling correction using Wigner's method	Rate constant with Wigner's method	Tunnelling correction using Eckart method	Rate constant with Eckart's method
$E \rightleftharpoons 9Z$	1.01	3.5497×10^3	1.01	3.5303×10^3
$E \rightleftharpoons 13Z$	1.01	1.9028×10^7	1.0	1.8896×10^7
$E \rightleftharpoons 15Z$	1.02	1.1060×10^7	1.02	1.1101×10^7

Table 9. Thermodynamic Parameters (in kcal mol⁻¹) of the all Interconversions at 298 K

	$E \rightleftharpoons 9Z$	$E \rightleftharpoons 13Z$	$E \rightleftharpoons 15Z$
ΔH_r	1.24(1.9) ^a	2.93(3.3) ^a	3.04(4.0) ^a
ΔG_r	1.30(1.6) ^a	1.94(1.7) ^a	2.68(1.3) ^a

^aB3LYP/6-31G(d) [14].

Temperature dependence of the Wigner's tunneling coefficients computed for the E \rightleftharpoons Z- β -carotenes is plotted in Fig. 7.

Interconversions

The thermodynamic parameters, such as enthalpy and Gibbs free energy, are calculated and reported in Table 9. According to data of ΔH_r and ΔG_r , all interconversions are endothermic and endergonic processes. Among them, 9Z would be thermodynamically more stable than 13Z and 15Z with $\Delta G_r = 1.24$ kcal mol⁻¹ and $\Delta H_r = 1.30$ kcal mol⁻¹. There is a good agreement between our thermodynamic data and Wen-HsinGuo.

CONCLUSIONS

The most stable isomer among the all-*E*- and *Z*- β -carotenes was all-*E* isomer. The converting process of all-*E* to three *Z*-isomers was endothermic. The conversion of the isomers to the 13*Z*-isomer was performed better in the studied temperature range. The conversion of *E*- to 9*Z*-isomer is about 10⁴ times slower than that for the other two isomers.

ACKNOWLEDGEMENTS

This work was supported by the Sistan and Baluchestan University.

REFERENCES

- [1] Belitz, I. H. D.; Grosch, I. W., Food Chemistry. Springer Science & Business Media, 2013, pp. 234-245.
- [2] Wong, D. W., Mechanism and Theory in Food Chemistry. Springer, 1989, pp. 380-500.
- [3] Zepka, L. Q.; Jacob-Lopes, E.; De Rosso, V. V., Progress in Carotenoid Research. IntechOpen, 2018, pp. 1-13.
- [4] Dutta, D.; Chaudhuri, U. R.; Chakraborty, R., Structure, health benefits, antioxidant property and processing and storage of carotenoids. *Afr. J. Biotechnol.* **2005**, *4*, DOI: 10.5897/AJB2005.000-3278.
- [5] Kaczor, A.; Baranska, M., Carotenoids: Nutrition, Analysis and Technology. John Wiley & Sons, 2016, pp. 1-100.
- [6] Alvarez, R.; Vaz, B.; Gronemeyer, H.; de Lera, A. R., Functions, therapeutic applications, and synthesis of retinoids and carotenoids. *Chem. Rev.* **2014**, *114*, 1-125, DOI: 10.1021/cr400126u.
- [7] G Britton, B.; Liaaen, S.; H Pfander, P., Carotenoids, Nutrition and Health. Springer, 2019, pp. 1-50.
- [8] Galano, A., Relative antioxidant efficiency of a large series of carotenoids in terms of one electron transfer reactions. *J. Phys. Chem. B* **2007**, *111*, 12898-12908, DOI: 10.1021/jp074358u.
- [9] Saini, R. K.; Keum, Y. -S., Carotenoid extraction methods: A review of recent developments. *Food Chem.* **2018**, *240*, 90-103, DOI: 10.1016/j.foodchem.2017.07.099.
- [10] Landrum, J. T., Carotenoids: Physical, Chemical, and Biological Functions and Properties. CRC Press, 2009, pp. 229-250.
- [11] Boon, C. S.; McClements, D. J.; Weiss, J.; Decker, E. A., Factors influencing the chemical stability of carotenoids in foods. *Crit. Rev. Food Sci. Nutr.* **2010**, *50*, 515-532, DOI: 10.1080/10408390802565889.
- [12] Preedy, V. R., Vitamin A and Carotenoids: Chemistry, Analysis, Function and Effects. Royal

- Society of Chemistry, 2012, pp. 129-158.
- [13] Kiokias, S.; Proestos, C.; Varzakas, T., A review of the structure, biosynthesis, absorption of carotenoids-analysis and properties of their common natural extracts. *Curr. Res. Nutr. Food Sci.* **2016**, *4*, 25-37, DOI: 10.12944/CRNFSJ.4.Special-Issue1.03.
- [14] Guo, W. H.; Tu, C. Y.; Hu, C. H., *Cis-trans* isomerizations of β -carotene and lycopene: A theoretical study. *J. Phys. Chem. B* **2008**, *112*, 12158-12167, DOI: 10.1021/jp8019705.
- [15] Qiu, D.; Chen, Z. -R.; Li, H. -R., Density functional theory study on thermal isomerization of β -carotene. *J. Mol. Struct.* **2008**, *865*, 44-48, DOI: 10.1016/j.theochem.2008.06.015
- [16] Bernardi, B. F.; Garavelli, M.; Olucchi, M., *Trans-cis* isomerization in long linear polyenes as beta-carotene models: a comparative CAS-PT2 and DFT study. *Mol. Phys.* **1997**, *92*, 359-364, DOI: 10.1080/002689797170095.
- [17] Schlücker, S.; Szeghalmi, A.; Schmitt, M.; Popp, J.; Kiefer, W., Density functional and vibrational spectroscopic analysis of β -carotene. *J. Raman Spectrosc.* **2003**, *34*, 413-419, DOI: 10.1002/jrs.1013.
- [18] Cerón-Carrasco, J. P.; Requena, A.; Marian, C. M., Theoretical study of the low-lying excited states of β -carotene isomers by a multireference configuration interaction method. *Chem. Phys.* **2010**, *373*, 98-103, DOI: 10.1016/j.chemphys.2010.02.011.
- [19] Von Doering, W.; Sotiriou-Leventis, C.; Roth, W., Thermal interconversions among 15-*cis*-, 13-*cis*- and all-*trans*- β -carotene: kinetics, Arrhenius parameters, thermochemistry, and potential relevance to anticarcinogenicity of all-*trans*- β -carotene. *J. Am. Chem. Soc.* **1995**, *117*, 2747-2757, DOI: 10.1021/ja00115a010.
- [20] Ceron-Carrasco, J.; Bastida, A.; Zuniga, J.; Requena, A.; Miguel, B., Density functional theory study of the stability and vibrational spectra of the β -carotene isomers. *J. Phys. Chem. A* **2009**, *113*, 9899-9907, DOI: 10.1021/jp9037446.
- [21] Colle, I. J.; Lemmens, L.; Knockaert, G.; Van Loey, A.; Hendrickx, M., Carotene degradation and isomerization during thermal processing: a review on the kinetic aspects. *Crit. Rev. Food Sci. Nutr.* **2016**, *56*, 1844-1855, DOI: 10.1080/10408398.2013.790779.
- [22] Xiao, Y. D.; Huang, W. Y.; Li, D. J.; Song, J. F.; Liu, C. D.; Wei, Q. Y.; Zhang, M.; Yang, Q. M., Thermal degradation kinetics of all-*trans* and *cis*-carotenoids in a light-induced model system. *Food Chem.* **2018**, *239*, 360-368, DOI: 10.1016/j.foodchem.2017.06.107.
- [23] Knockaert, G.; Pulissery, S. K.; Lemmens, L.; Van Buggenhout, S.; Hendrickx, M.; Van Loey, A., Carrot β -carotene degradation and isomerization kinetics during thermal processing in the presence of oil. *J. Agric. Food Chem.* **2012**, *60*, 10312-10319, DOI: 10.1021/jf3025776.
- [24] Zhao, Y.; Truhlar, D. G., The M06 suite of density functionals for main group thermochemistry, thermochemical kinetics, noncovalent interactions, excited states, and transition elements: two new functionals and systematic testing of four M06-class functionals and 12 other functionals. *Theor. Chem. Acc.* **2008**, *120*, 215-241, DOI: 10.1007/s00214-007-0310-x.
- [25] Montgomery Jr, J.; Ochterski, J.; Petersson, G., A complete basis set model chemistry. IV. An improved atomic pair natural orbital method. *J. Chem. Phys.* **1994**, *101*, 5900-5909, DOI: 10.1063/1.467306.
- [26] Zhao, Y.; Truhlar, D. G., Hybrid meta density functional theory methods for thermochemistry, thermochemical kinetics, and noncovalent interactions: The MPWB1B95 and MPWB1K models and comparative assessments for hydrogen bonding and van der Waals interactions. *J. Phys. Chem. A* **2004**, *108*, 6908-6918, DOI: 10.1021/jp048147q.
- [27] Mardirossian, N.; Head-Gordon, M., How accurate are the Minnesota density functionals for noncovalent interactions, isomerization energies, thermochemistry, and barrier heights involving molecules composed of main-group elements. *J. Chem. Theory Comput.* **2016**, *12*, 4303-4325, DOI: 10.1021/acs.jctc.6b00637.
- [28] Rayne, S.; Forest, K., A comparative examination of density functional performance against the ISOL24/11 isomerization energy benchmark. *Comput. Theor. Chem.* **2016**, *1090*, 147-152, DOI: 10.1016/j.comptc.2016.06.018.
- [29] Zhao, Y.; Truhlar, D. G., Density functionals with

- broad applicability in chemistry. *Acc. Chem. Res.* **2008**, *41*, 157-167, DOI: 10.1021/ar700111a.
- [30] Zhao, Y.; Truhlar, D. G., Applications and validations of the Minnesota density functionals. *Chem. Phys. Lett.* **2011**, *502*, 1-13, DOI: 10.1016/j.cplett.2010.11.060.
- [31] Park, H. S.; Kang, Y. K., Which DFT levels of theory are appropriate in predicting the prolyl *cis-trans* isomerization in solution? *New. J. Chem.* **2019**, *43*, 17159-17173, DOI:https://10.1039/C9NJ02946J.
- [32] Dibble, T. S.; Sha, Y.; Thornton, W. F.; Zhang, F., *Cis-trans* isomerization of chemically activated 1-methylallyl radical and fate of the resulting 2-buten-1-peroxy radical. *J. Phys. Chem. A* **2012**, *116*, 7603-7614, DOI: 10.1021/jp303652x.
- [33] Wigner, E., Concerning the excess of potential barriers in chemical reactions. *Z. Phys. Chem. B Chem. E* **1932**, *19*, 203-216, DOI:
- [34] Eckart, C., The penetration of a potential barrier by electrons. *Phys. Rev.* **1930**, *35*, 1303, DOI: 10.1103/PhysRev.35.1303.
- [35] Canneaux, S.; Bohr, F.; Henon, E., KiSTheLP: A program to predict thermodynamic properties and rate constants from quantum chemistry results. *J. Comput. Chem.* **2014**, *35*, 82-93, DOI: 10.1002/jcc.23470.
- [36] Luchini, G.; Alegre-Requena, J.; Funes-Ardoiz, I.; Paton, R., GoodVibes: Automated thermochemistry for heterogeneous computational chemistry data. *F1000Research* **2020**, *9*, DOI: 10.12688/f1000research.22758.1.
- [37] Blanquart, G., Effects of spin contamination on estimating bond dissociation energies of polycyclic aromatic hydrocarbons. *Int. J. Quantum Chem.* **2015**, *115*, 796-801, DOI: 10.1002/qua.24904.
- [38] Glasstone, S.; Laidler, K. J.; Eyring, H., *The Theory of Rate Processes: The Kinetics of Chemical Reactions, Viscosity, Diffusion and Electrochemical Phenomena.* McGraw-Hill Book Company, Incorporated, 1941, p. 10-100.
- [39] Laidler, K. J.; King, M. C., Development of transition-state theory. *J. Phys. Chem.* **1983**, *87*, 2657-2664, DOI: 10.1021/j100238a002.